coatings

Article

Fabrication of Fe_3O_4@SiO_2 Nanofluids with High Breakdown Voltage and Low Dielectric Loss

Bin Du *, Yu Shi and Qian Liu

School of Electrical Engineering and Automation, Hefei University of Technology, Hefei 230009, China; hf45578@163.com (Y.S.); hf65518@163.com (Q.L.)

* Correspondence: dubin@hfut.edu.cn

Received: 20 September 2019; Accepted: 25 October 2019; Published: 1 November 2019

Abstract: Insulating oil modified by nanoparticle (often called nanofluids) has recently drawn considerable attention, especially concerning the improvement of electrical breakdown and thermal conductivity of the nanofluids. However, traditional insulating nanofluid often tends to high dielectric loss, which accelerates the ageing of nanofluids and limits its application in electrical equipment. In this paper, three core-shell Fe_3O_4@SiO_2 nanoparticles with different SiO_2 shell thickness were prepared and subsequently dispersed into insulating oil to achieve nanofluids. The dispersion stability, breakdown voltages and dielectric properties of these nanofluids were comparatively investigated. Experimental results show the alternating current (AC) and positive lightning breakdown voltage of nanofluids increased by 30.5% and 61%, respectively. Moreover, the SiO_2 shell thickness of Fe_3O_4@SiO_2 nanoparticle had significant effects on the dielectric loss of nanofluids.

Keywords: coating; core-shell; nanofluids; breakdown voltage; dielectric loss

1. Introduction

Adding well-dispersed nanoparticles into insulating oil can effectively improve the insulation properties and thermal conductivity of insulating oil [1,2]. The Fe_3O_4 nanoparticles have been proven to improve the AC and lightning breakdown voltage of insulating oil [3], and the insulation properties of nanofluids are determined by nanoparticle size, surfactant and structure [4]. The mechanism of Fe_3O_4 nanoparticle effect on the breakdown voltage was studied at a certain level. It was found that nanoparticles can inhibit space charge accumulation and uniform electric field in insulating oil [5]. Several studies have shown that nanoparticles increase the trapping density and depth, and reduce the velocity of streamer propagation in nanofluids [6,7].

Dielectric loss factor is a key parameter for insulating nanofluids. In fact, many high breakdown voltage nanofluids have been prepared but they tend to have high dielectric loss [8], especially for nanoparticles with high relative permittivity. For instance, the relative permittivity of Fe_3O_4 nanoparticles is 80 [9], much higher than that of insulating oil, and this will lead to a significant increase in polarization loss of insulating oil. Therefore, how to prepare high breakdown voltage nanofluids with low dielectric loss factor is a very interesting topic.

At present, a lot of researches have been carried out on the synthesis of nanoparticles with different sizes and morphologies [10,11]. Grzelczak et al. shows the preparation methods of gold nanoparticles with different sizes [12], and it has been proven that the nanoparticle size and morphology have an important effect on the dielectric properties of materials [13,14]. However, it is difficult for a single nanoparticle to meet the requirements of increasing breakdown voltage and reducing dielectric loss of insulating oil. Core-shell structure nanoparticles show great potential for fabricating nanocomposites, because of their unique properties, such as high thermal conductivity, large surface area and special dielectric properties. Li et al. prepared insulating rPANI@rGO nanocomposites by an in situ polymerization method with high dielectric constant and low dielectric loss [15]. Grumezescu et al. reported Fe_3O_4-oleic acid–usnic acid core-shell–extra-shell nanofluids could have application for different medical devices [16]. However, most of the works ignored the influences of core-shell nanoparticle size on the dielectric properties of nanofluids, and the method of prepared nanofluids with high breakdown voltage and low dielectric loss still has never been reported.

This paper researches the effect of Fe_3O_4@SiO_2 nanoparticles on the insulation properties and dielectric loss of insulating oil. The insulating nanofluids were prepared by adding three different sizes of Fe_3O_4@SiO_2 nanoparticles; thereafter the breakdown voltages and dielectric properties of nanofluids were presented and discussed. The Fe_3O_4@SiO_2 nanofluids showed high insulation performance as well as low dielectric loss factor, which indicates significant application in the power industry.

2. Experimental

2.1. Preparation of Nanofluids

The process of preparation of Fe_3O_4@SiO_2 nanoparticles is shown in Figure 1. The Fe_3O_4@SiO_2 nanofluids were obtained via four main procedures: Preparation of Fe_3O_4 nanoparticle, preparation of the Fe_3O_4@SiO_2 nanoparticles, modification of Fe_3O_4@SiO_2 nanoparticles and synthesis of the Fe_3O_4@SiO_2 nanofluids.

- Fe_3O_4 nanoparticles: Fe_3O_4 nanoparticles were prepared by coprecipitation method. A total of 5.4 g of iron (III) chloride hexahydrate and 3.9 g of iron (II) chloride tetrahydrate was mixed in 100 mL of deionized water. The obtained solution was slowly added by 25 mL of ammonia with string at 60 °C for 12 h. The precipitated iron oxide was washed twice with deionized water. The black powder was subsequently dried in vacuum at 70 °C for 24 h.
- Fe_3O_4@SiO_2 nanoparticles: A total of 3.0 g of iron oxide was dispersed into 500 mL of ethanol and ultrasonic treated for 1 h at room temperature, then 2, 4, and 8 mL of tetraethyl orthosilicate (TEOS) were added to the mixtures to obtain Fe_3O_4@SiO_2 nanoparticles with different SiO_2 shell thickness. The nanoparticles were subsequently centrifuged and washed several times.
- Modification of Fe_3O_4@SiO_2 nanoparticles: A total of 2.0 g of Fe_3O_4@SiO_2 nanoparticle was dissolved in 300 mL of ethanol, and 0.1 g of oleic acid was then added to the mixture under mechanical agitation for 1 h. After that, the product was washed by ethanol and dried at 60 °C for 24 h.
- Preparation of nanofluids: The three Fe_3O_4@SiO_2 nanoparticles were dispersed into a type of insulating oil, the FR3 mechanized from Cargill, by ultrasonic treatment. They were tagged as sample A, B, and C, respectively. Before the electrical performance test, the three nanofluids and the FR3 were dried at 85 °C under 50 Pa for 72 h to reduce the water content of samples below 60 mg/kg.

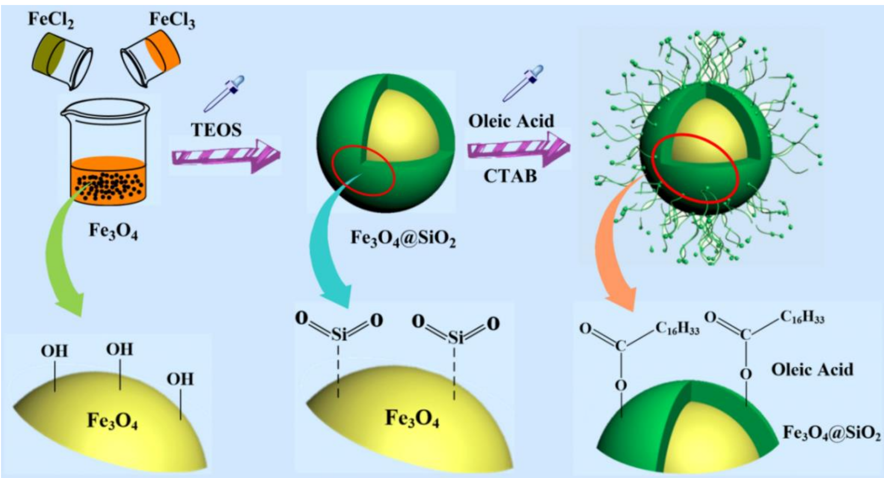

Figure 1. The schematic of the preparation of Fe_3O_4@SiO_2 nanoparticle.

2.2. Nanoparticle Characterization

The morphologies of the three different sized nanoparticles prepared by adding different amounts of TEOS were characterized by transmission electron microscopy (TEM, JEM-2100F, Japan Electronics Ltd., Tokyo, Japan), as shown from Figure 2(A1–C1). The polydispersity of the three different sized nanoparticle were tested by Zeta potential size analyzer (MS-2000, Malvern Panalytical Ltd., Melvin, UK), and the results are shown in Figure 2(A2–C2). It is seen that the prepared nanoparticles are monodispersed spherical particles, and each nanoparticle is composed of two distinct regions. The darker central-core is the Fe_3O_4 crystal, and the surrounding layer is low density shell of SiO_2. The Fe_3O_4 nanoparticles coated with SiO_2 can effectively avoid the agglomeration of the nanoparticle. It also can be seen that the size distributions of the three nanoparticles are narrow, indicating the three Fe_3O_4@SiO_2 are uniform nanoparticles. Meanwhile, the nanoparticle sizes tested by Zeta potential analyzer are basically the same as those observed by TEM.

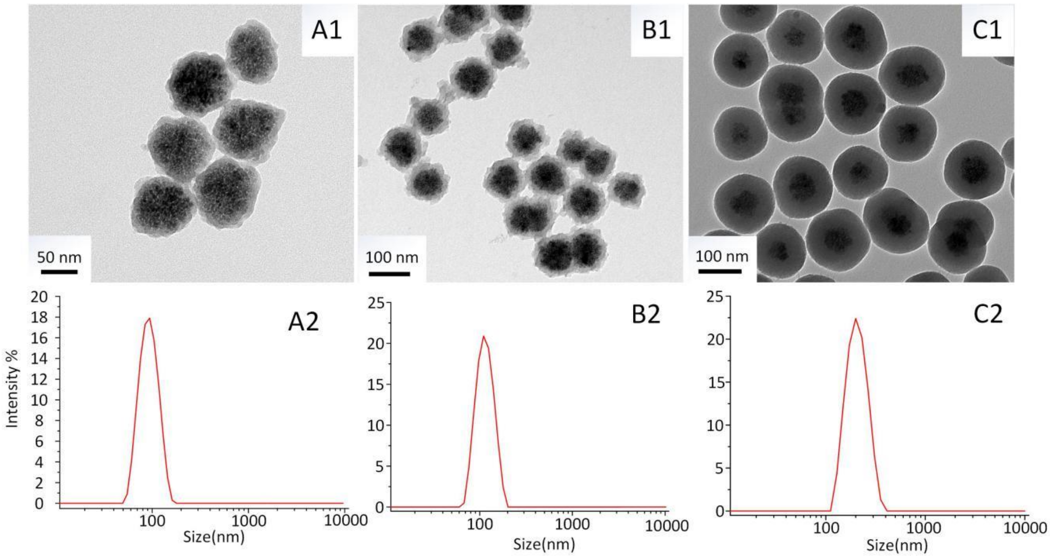

Figure 2. TEM images and size distribution of Fe_3O_4@SiO_2 nanoparticle prepared with different amounts of tetraethyl orthosilicate (TEOS). 2 mL of TEOS: (**A1**) TEM images and (**A2**) size distribution; 4 mL of TEOS: (**B1**) TEM images and (**B2**) size distribution; 8 mL of TEOS: (**C1**) TEM images and (**C2**) size distribution.

As the amounts of TEOS increase, the thickness of the SiO_2 shells increase continuously. The SiO_2 shells vary in thickness from ~7.5 nm (Figure 2(A1)) to ~50 nm (Figure 2(C1)) via ~24 nm (Figure 2(B1)). However, the sizes of the Fe_3O_4 cores do not change significantly, which are always ~60 nm.

Figure 3 depicts the Fourier-transform infrared spectroscopy (FTIR, Nicolet, Thermo Electron Corporation, Franklin, TN, USA) spectra of the obtained nanoparticle samples. In the spectrum, the stretching vibration absorption of Si–O bands appears at 466, 801 cm^{-1} and the stretching vibration absorption of Fe–O emerges at 568 cm^{-1} in the spectrum. These absorption peaks prove that the Fe_3O_4@SiO_2 nanoparticle was synthesized. Furthermore, C–O stretching vibration absorption at 1100 cm^{-1} was found in this spectrum, and the wide absorption peak at 3485 cm^{-1} represents the –OH group. The above results indicate that the oleic acid molecules were successfully bonded onto surfaces of the Fe_3O_4@SiO_2 nanoparticles. The surface modification of Fe_3O_4@SiO_2 nanoparticles by oleic acid can improve the dispersion stability of nanoparticle in insulating oil.

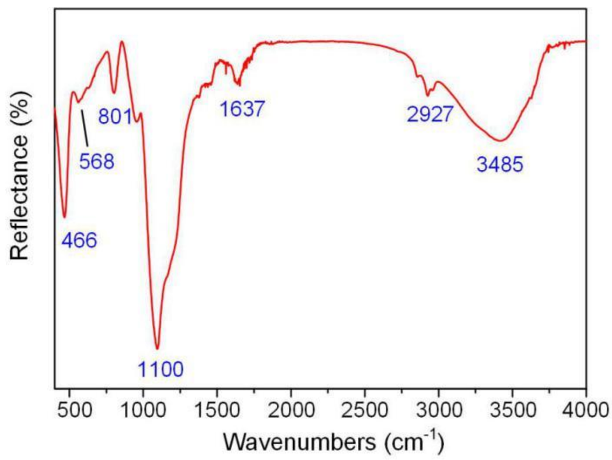

Figure 3. FTIR spectra of obtained Fe_3O_4@SiO_2 nanoparticle samples.

3. Results and Discussion

3.1. Dispersion Stability of Nanofluids

The long-term dispersion stability of Fe_3O_4@SiO_2 nanoparticles in insulating oil was characterized by natural deposition method. In Figure 4, three nanofluids with a much larger nanoparticle/oil weight ratio (0.1%) were set for 90 days in ambient condition to examine their storage-time dependent dispersion stability. The FR3 oil was also measured for comparison. It can be seen that there was no agglomeration and precipitation in the nanofluids, indicating that the nanofluids have good dispersion stability.

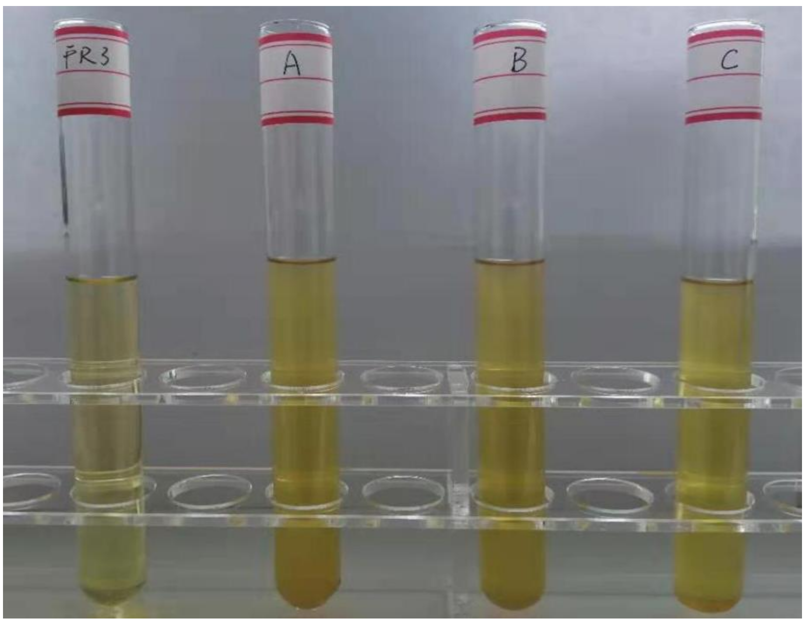

Figure 4. FR3 and three types nanofluids. (**A**) FR3 oil used as a comparison sample; (**B**) Sample A: FR3 oil was added to 0.1 wt % Fe_3O_4@SiO_2 nanoparticles, and the nanoparticles were prepared with 2 mL of TEOS; (**C**) Sample B: 4 mL of TEOS; (**D**) Sample C: 8 mL of TEOS.

3.2. Breakdown Voltage of Nanofluids

The AC and lightning breakdown voltages of FR3 oil and three nanofluids were measured in accordance with IEC 60,156 and IEC 60,897 [17,18]. A ball-plate steel electrode was adopted for the AC breakdown voltage test and the electrode gap was 2.5 nm. The device for testing the lightning breakdown voltage is shown in Figure 5. This device was composed of a steel electrode and a container. The high voltage electrode was a steel needle, and the ground electrode was a 13 mm-diameter ball. The gap distance between high voltage electrode and grounding electrode was 15 mm. Standard lightning impulse of 1.2 (±30%)/50 μs (±20%) with both negative and positive polarities were applied to all samples.

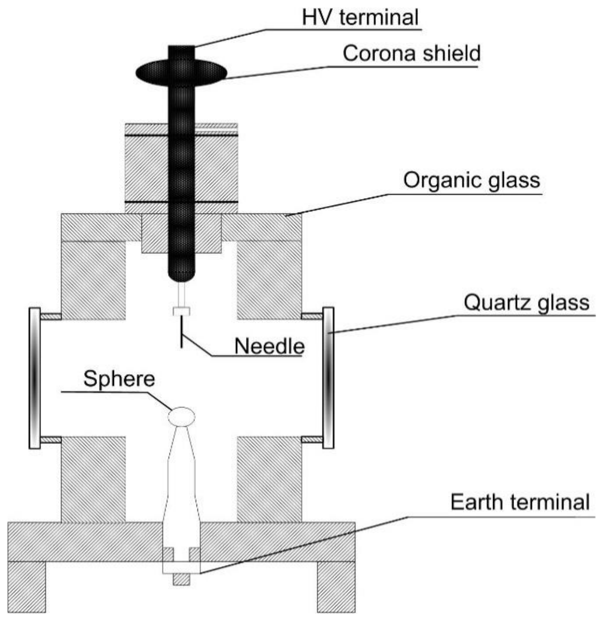

Figure 5. Sketch of electrode setup for lightning breakdown experiments.

Figure 6 shows the measurement results of AC breakdown voltages of FR3 oil and three sizes of nanofluids at different nanoparticle contents. The FR3 oil was marked as the sample with 0 ppm Fe_3O_4@SiO_2 nanoparticles added. All the measurements were made on five oil samples. It was seen that the AC breakdown voltages of each nanofluid increases to a top value and decreases afterwards with higher nanoparticle content. For example, the AC breakdown voltage enhanced by 30.5% from 52.1 kV for FR3 to 68.0 kV for nanofluids C that was added with 100 ppm Fe_3O_4@SiO_2 nanoparticle.

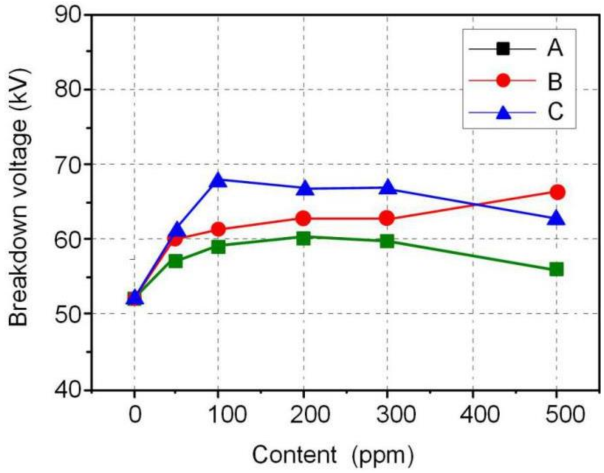

Figure 6. Influence of contents of Fe_3O_4@SiO_2 on the AC breakdown voltage of the nanofluids. (**A**) Sample A: FR3 oil was added to Fe_3O_4@SiO_2 nanoparticles prepared with 2 mL of TEOS; (**B**) Sample B: 4 mL of TEOS; (**C**) Sample C: 8 mL of TEOS.

The positive and negative lightning breakdown voltages of oil samples are summarized in Figures 7 and 8. The positive lightning breakdown voltage of nanofluids provides significant effects, but for negative lightning breakdown voltage the attained improvement is insignificant. Here the positive lightning leads to strongly increased breakdown voltages. For example, nanofluids A, which contained 300 ppm nanoparticles, shows the highest breakdown voltage of 68.5 kV, which is significantly higher voltage compared to the 42.4 kV for FR3 oil, improved by about 61%. However, the negative breakdown voltage of nanofluids was not significantly increased. As the Fe_3O_4@SiO_2 nanoparticle content was 200 ppm, the breakdown voltage of nanofluids A was 6.9% higher than that of FR3 oil. This is mainly due to the different nanoparticle activities in oil under different polarity electric fields, leading to different impacts of the positive and negative lightning breakdown voltage of nanofluids [19].

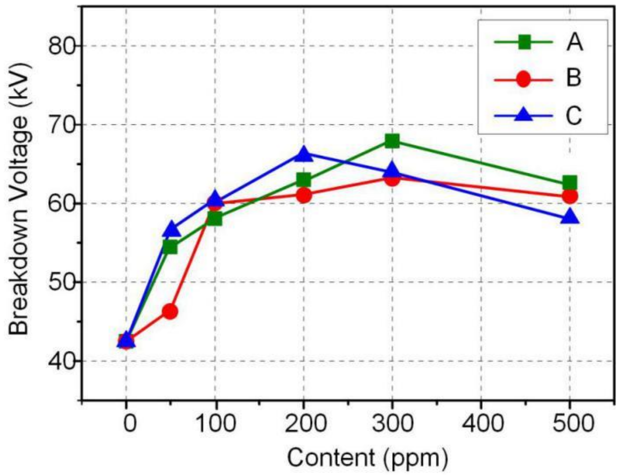

Figure 7. Influence of contents of nanoparticle on the positive lightning breakdown voltage of nanofluids. (**A**) Sample A: FR3 oil was added to Fe_3O_4@SiO_2 nanoparticles prepared with 2 mL of TEOS; (**B**) Sample B: 4ml of TEOS; (**C**) Sample C: 8 mL of TEOS.

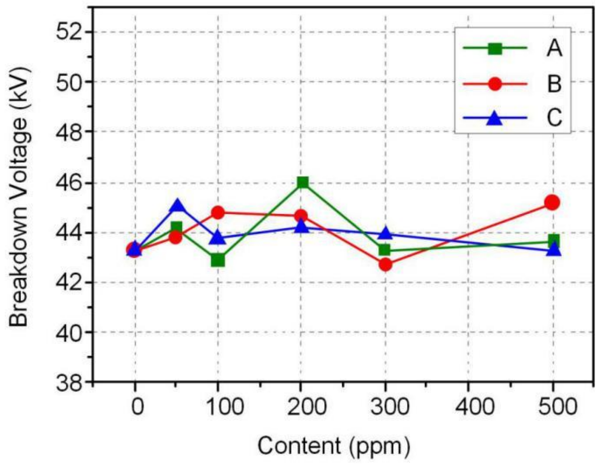

Figure 8. Influence of contents of nanoparticle on the negative lightning breakdown voltage of nanofluids. (**A**) Sample A: FR3 oil was added to Fe_3O_4@SiO_2 nanoparticles prepared with 2 mL of TEOS; (**B**) Sample B: 4 mL of TEOS; (**C**) Sample C: 8 mL of TEOS.

3.3. Dielectric Properties of Nanofluids

Figure 9 shows the curves of relative permittivity of FR3 oil and three nanofluids between 10^{-2} and 10^6 Hz. There is no visible difference among FR3 and three sizes of nanofluids at a frequency above 10 Hz. With frequency below 10 Hz, the relative permittivity of oil samples follows the sequence A > B > C > FR3. It is obvious that different thickness shells of Fe_3O_4@SiO_2 nanoparticle endow nanofluids with varied relative permittivity values. As is well known, the relative permittivity of Fe_3O_4 is about 80 [9], which is much greater than that of 3.9 for SiO_2 nanoparticle. According to the Maxwell–Garnett model [20], the relative permittivity of the $Fe_3O_4@SiO_2$ nanoparticle, ε_n, can be calculated by following formula:

$$\frac{\varepsilon_{\rm n}-\varepsilon_1}{\varepsilon_{\rm n}+2\varepsilon_1}=\varphi_v\frac{\varepsilon_2-\varepsilon_1}{\varepsilon_2+2\varepsilon_1} \tag{1}$$

where ε_1 = 3.9 and ε_2 = 80, the relative dielectric constant of SiO_2 and Fe_3O_4 nanoparticle, respectively, and φ_v is the Fe_3O_4 core volumetric concentration in the $Fe_3O_4@SiO_2$ nanoparticle. According to formula (1), the relative permittivity of $Fe_3O_4@SiO_2$ nanoparticles decreases rapidly with the increase of SiO_2 shell thickness.

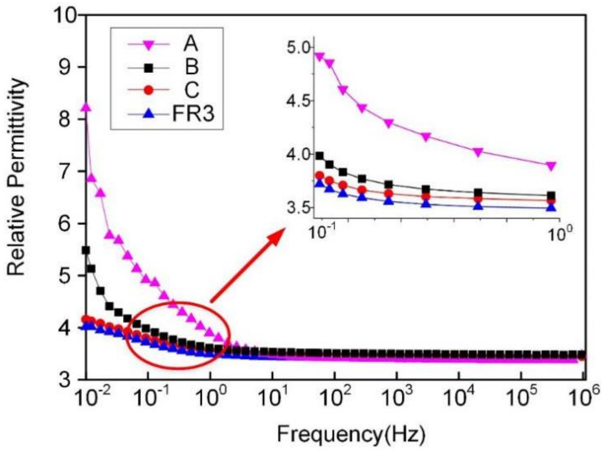

Figure 9. The relative permittivity of FR3 oil and three nanofluids at different frequencies. (**A**) Sample A: FR3 oil was added to $Fe_3O_4@SiO_2$ nanoparticles prepared with 2 mL of TEOS; (**B**) Sample B: 4 mL of TEOS; (**C**) Sample C: 8 mL of TEOS.

Figure 10 gives the frequency dependence of dielectric loss factor for FR3 oil and three sizes of nanofluids. The curves of the dielectric loss factor show a decrease with increasing frequency and behave almost identically in the range of 1–10^7 Hz. However, the results present a difference between 10^{-2} Hz and 1 Hz. It can also be seen that the dielectric loss factor of nanofluids decreases with the increase of SiO_2 shell thickness. At a frequency of 0.1 Hz, the dielectric loss factor of 3% for nanofluids A is significantly higher than 0.5% for FR3 oil. However, the dielectric loss factor of the nanofluids C was only slightly increased.

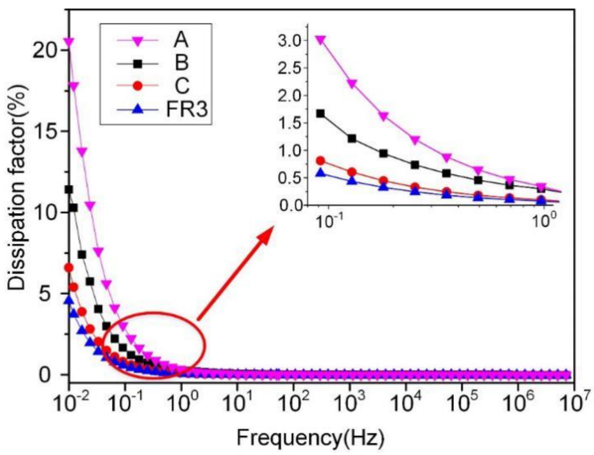

Figure 10. The dielectric loss factor of FR3 oil and three nanofluids at different frequencies. (**A**) Sample A: FR3 oil was added to $Fe_3O_4@SiO_2$ nanoparticles prepared with 2 mL of TEOS; (**B**) Sample B: 4 mL of TEOS; (**C**) Sample C: 8 mL of TEOS.

4. Conclusions

- In this work, core-shell $Fe_3O_4@SiO_2$ nanoparticles were synthesized. The TEM test showed the SiO_2 shell thickness increased with the increase of TEOS concentration. Zeta potential size test showed the three $Fe_3O_4@SiO_2$ were uniform nanoparticles.
- The nanofluids with high breakdown voltage and low dielectric loss were developed by dispersing $Fe_3O_4@SiO_2$ nanoparticles with different thicknesses of SiO_2 shell. The long-term dispersion stability of $Fe_3O_4@SiO_2$ nanoparticles in insulating oil was characterized by natural deposition method. The AC and positive lightning breakdown voltage of nanofluids were significantly improved compared with that of FR3 oil, but the improvement is not obvious for the negative lightning breakdown voltage.
- As the thickness of the SiO_2 shell increases, the relative dielectric constant and the dielectric loss factor decrease. When the SiO_2 shell is 50 nm, the dielectric loss factor of nanofluids is basically the same as that of FR3 oil. This work will be beneficial to the application of nanofluids in transformers.

Author Contributions: Conceptualization, B.D.; Methodology, B.D.; Investigation B.D. and Y.S.; Resources, B.D.; Data Curation, Q.L.; Writing—Original Draft Preparation, B.D., Y.S. and Q.L.; Writing-Review and Editing, B.D.; Funding Acquisition, B.D.

Funding: This work was financially supported by the National Natural Science Foundation of China (grant No. 51707052).

Acknowledgments: Thank Y.S. and Q.L. for their help.

Conflicts of Interest: The authors declare that they have no conflict of interest.

References

1. Choi, C.; Yoo, H.S.; Oh, J.M. Preparation and heat transfer properties of nanoparticle-in-transformer oil dispersions as advanced energy-efficient coolants. *Curr. Appl. Phys.* **2007**, *8*, 710–712. [CrossRef]
2. Yao, W.; Huang, Z.; Li, J.; Wu, L.; Xiang, C. Enhanced electrical insulation and heat transfer performance of vegetable oil based nanofluids. *J. Nanomater.* **2018**, *2018*, 4504208. [CrossRef]
3. Thabet, A.; Allam, M.; Shaaban, S.A. Investigation on enhancing breakdown voltages of transformer oil nanofluids using multi-nanoparticles technique. *Inst. Eng. Technol.* **2017**, *12*, 1171–1176.
4. Li, J.; Du, B.; Wang, F.; Yao, W.; Yao, S. The effect of nanoparticle surfactant polarization on trapping depth of vegetable insulating oil-based nanofluids. *Phys. Lett. A* **2016**, *380*, 604–608. [CrossRef]
5. Lv, Y.; Wang, Q.; Zhou, Y.; Li, C.; Ge, Y.; Qi, B. Effect of Fe_3O_4 nanoparticles on positive streamer propagation in transformer oil. *AIP Adv.* **2016**, *6*, 035110. [CrossRef]
6. Takada, T.; Hayase, Y.; Tanaka, Y.; Okamoto, T. Space charge trapping in electrical potential well caused by permanent and induced dipoles. *Annu. Rep. Conf. Electr. Insul. Dielectr. Phenom.* **2008**, *15*, 152–160. [CrossRef]
7. Du, Y.; Lv, Y.; Li, C.; Chen, M.; Zhong, Y.; Zhang, S.; Zhou, Y. Effect of nanoparticles on charge transport in nanofluid-impregnated pressboard. *J. Appl. Phys.* **2012**, *111*, 1243221. [CrossRef]
8. Lanje, A.S.; Sharma, S.J.; Ningthoujam, R.S.; Ahn, J.S.; Pode, R.B. Low temperature dielectric studies of zinc oxide (ZnO) nanoparticles prepared by precipitation method. *Adv. Powder Technol.* **2013**, *24*, 331–335. [CrossRef]
9. Hwang, J.G.; Zahn, M.; O'Sullivan, F.M.; Pettersson, L.A.; Hjortstam, O.; Liu, R. Effects of nanoparticle charging on streamer development in transformer oil-based nanofluids. *J. Appl. Phys.* **2010**, *107*, 014310. [CrossRef]
10. Mozaffari, S.; Li, W.; Dixit, M.; Seifert, S.; Lee, B.; Kovarik, L.; Mpourmpakis, G.; Karim, A.M. The role of nanoparticle size and ligand coverage in size focusing of colloidal metal nanoparticles. *Nanoscale Adv.* **2019**, *1*, 4052–4066. [CrossRef]
11. Li, W.; Ivanov, S.; Mozaffari, S.; Shanaiah, N.; Karim, A.M. Palladium acetate trimer: Understanding its ligand-induced dissociation thermochemistry using isothermal titration calorimetry, X-ray absorption fine structure, and ^{31}P nuclear magnetic resonance. *Organometallics* **2019**, *38*, 451–460. [CrossRef]

12. Grzelczak, M.; Pérez-Juste, J.; Mulvaney, P.; Liz-Marzán, L.M. Shape control in gold nanoparticle synthesis. *Chem. Soc. Rev.* **2008**, *37*, 1783–1791. [CrossRef] [PubMed]
13. Yu, G.; Cheng, Y.; Zhang, X. The dielectric properties improvement of cable insulation layer by different morphology nanoparticles doping into LDPE. *Coatings* **2019**, *9*, 204. [CrossRef]
14. Tkach, A.; Santos, A.; Zlotnik, S.; Serrazina, R.; Okhay, O.; Bdikin, I.; Costa, M.E.; Vilarinho, P. Strain-mediated substrate effect on the dielectric and ferroelectric response of potassium sodium niobate thin films. *Coatings* **2018**, *8*, 449. [CrossRef]
15. Li, M.; Huang, X.; Wu, C.; Xu, H.; Jiang, P.; Tanaka, T. Fabrication of two-dimensional hybrid sheets by decorating insulating PANI on reduced graphene oxide for polymer nanocomposites with low dielectric loss and high dielectric constant. *J. Mater. Chem.* **2012**, *22*, 23477–23484. [CrossRef]
16. Grumezescu, A.M.; Saviuc, C.; Chifiriuc, M.C.; Hristu, R.; Mihaiescu, D.E.; Balaure, P.; Stanciu, G.; Lazar, V. Inhibitory activity of Fe_3O_4/Oleic acid/usnic acid-core/shell/extra-shell nanofluid on S. aureus biofilm development. *IEEE Trans. Nanobiosci.* **2011**, *10*, 269–274. [CrossRef] [PubMed]
17. *IEC 60156: 2018. Insulating Liquids—Determination of the Breakdown Voltage at Power Frequency*; IEC: Geneva, Switzerland, 2018.
18. *IEC 60897: 2018. Methods for the Determination of the Lightning Breakdown Voltage of Insulating Liquids*; IEC: Geneva, Switzerland, 2018.
19. Li, J.; Zhang, Z.; Zou, P. Preparation of a vegetable oil-based nanofluid and investigation of its breakdown and dielectric properties. *IEEE Electr. Insul. Mag.* **2012**, *28*, 43–50. [CrossRef]
20. Miao, J.; Dong, M.; Ren, M.; Wu, X.; Shen, L.; Wang, H. Effect of nanoparticle polarization on relative permittivity of transformer oil-based nanofluids. *J. Appl. Phys.* **2013**, *113*, 204103. [CrossRef]